

Chemistry Analysis of Crud in Fuel Cladding under Various Heat Flux Conditions

Yunju Lee, Junhyuk Ham, Seung Chang Yoo, Dae Hyeon Park, Ji Hyun Kim*

Department of Nuclear Engineering, School of Mechanical, Aerospace, and Nuclear Engineering, Ulsan National Institute of Science and Technology (UNIST)

*Corresponding author: kimjh@unist.ac.kr

1. Introduction

Axial Offset Anomaly (AOA) is phenomenon which happened due to unexpected power shifts in reactor core. In Pressurized Water Reactor (PWR), since 1960, AOA has been observed and affect on economics and safety of power plants. [1]

AOA is known to be provoked by corrosion product deposits on fuel cladding, which is called crud. Crud has been known to composed of nickel and iron oxide species and its combination of boron species such as, nickel metal (Ni), nickel oxide (NiO), iron metal (Fe), magnetite (Fe₃O₄), nickel ferrite (NiFe₂O₄) and bonaccordite (Ni₂FeBO₅). Crud deposits on the fuel cladding surface through nucleate boiling and shows porous media. This porous structure changes the thermohydraulic behavior near cladding surface provoking precipitation of ions dissolved in coolant, such as boron and lithium. The boron, which accumulated on cladding surface, has high neutron capture cross section and affects on neutron transfer behavior near fuel cladding. From previous studies it is found that AOA occurred PWR have common characteristics, some degree of nucleate boiling on the fuel cladding, this indicates that the deposition of corrosion products by nucleate boiling is a root cause of AOA phenomenon.[2] To predicting the occurrence of AOA and its effects, crud formation and its properties must be investigated.

In this study, crud deposition experiments have been conducted, with variation of heat flux at cladding in high metal ion concentration. To investigate the effect of heat flux condition, three different experiment were performed at different heat flux conditions. Structure information of each specimen is analyzed by scanning Electron Microscopy (SEM) with Focused Ion Beam (FIB) instrument. And its chemical composition is investigated by Electron Dispersed Spectroscopy (EDX).

2. Experimental Methods

2.1. Experimental condition

Crud deposition experiments were performed in simulated PWR primary water with various heat flux condition 46 kW/m², 100 kW/m² and 150 kW/m². Three major conditions should be satisfied to simulate the crud deposition at reactor core; Nucleate boiling at cladding surface, existence of corrosion product in the primary water, and dissolved boron and lithium species in the primary water.

Table 1. Experimental conditions of crud deposition experiment with low hear flux condition.

Experimental condition	T2-1	T2-2	T2-3
Heat flux at specimen [kW/m ²]	46	100	150
Surface temperature of specimen [°C]	350.4	349.4 ~ 354.5	350.2 ~ 375.5
Average mass flux [kg/s]	0.01	0.015	0.018
Average coolant temperature [°C]	318 ~ 330	305 ~ 315	220 ~ 250
Effective full power day [day]	7		
Length of specimen [mm]	300		
Outer diameter of specimen [mm]	9.5		
Inner diameter of specimen [mm]	8.34		
Pressure [MPa]	15.5		
DH concentration [ppm]	2.7		
DO concentration [ppb]	~ < 5		
pH [ppm]	6.9 ~ 7.4		
Boron concentration [ppm]	1200		
Lithium concentration [ppm]	2.2		
Nickel concentration [ppm]	25		
Iron concentration [ppm]	12		

The heat flux condition on cladding specimen surface is simulated by using direct current heating method. The corrosion product dissolved in primary water, is simulated by dissolving Ni, Fe ions with nickel acetate and Fe Ethylenediaminetetraacetic acid (EDTA). To accelerate the crud deposition, concentrated metal ion solutions were used. The crud deposition experiments were conducted for 7 days.

Considering the pH recommendation in PWR primary water, boron and lithium concentration was determined to 1200 ppm and 2.2 ppm respectively. Thus, pH was being kept to 6.9~7.4.

To observe temperature change in cladding surface, a thermocouple is spot welded at inner surface of the specimen.

2.2. Analysis strategy

After the experiment, visual inspection was conducted for the entire specimen to observe macroscopic characteristic of crud deposition behavior. For specified structure analysis, microscopic observation was conducted with FIB-SEM instrument.

SEM was performed for both surface and cross section of the specimens. Cross section planes were

trimmed by FIB. To investigate chemical composition of crud, EDX was also conducted for cross section plane of each specimen during SEM analysis. Upper 7 cm of area of each specimen are compared in this paper.

3. Results and discussion

3.1. Structure and chemistry analysis of T2-1 top region

SEM surface image was taken from Top specimen to check its morphology. The chimney-like structure was also found from the SEM surface images in Fig.5. Because most of the large surface chimneys (or pore) have small chimneys (or pores) in it, it is hard to define a chimney size and shape.

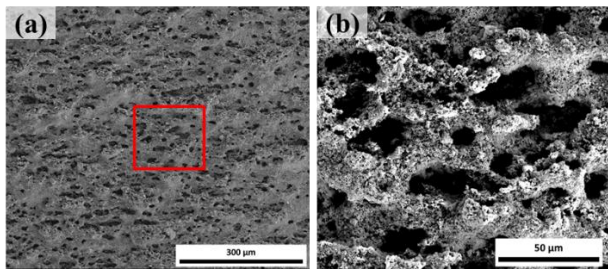


Fig. 1 SEM surface image of T2-1 Top specimen. A small region of (a) which indicated with red box is magnified and showed in (b).

To observe the shape of the crud layer in radial direction cross-section of the specimen is made by FIB in perpendicular with an axial direction of the tube. The SEM image of Cross-section plane is obtained in Fig. 1 and point EDX results are summarized in Table 2. The cross-section image shows that crud is formed on the rigid ZrO₂ layer. The maximum thickness of the crud in the FIB spot of Top specimen was 64.34 μm and the minimum thickness is 44.21 μm. Average crud thickness is 56.82 μm with a standard deviation of 6.07.

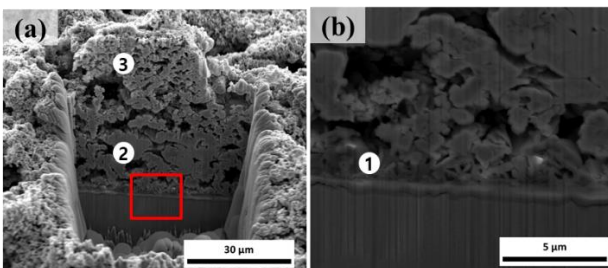


Fig. 2 SEM cross section image of T2-1 Top specimen. A red-boxed region in (a) is magnified and shown in (b).

Tale 2. Point EDX analysis of the points in Fig. 2 in a.t.%

Point	O	Fe	Ni	Zr	Ni/Fe ratio
1	64.2	9.9	4.5	21.4	0.46

2	55.1	22.3	12.6	10.0	0.57
3	64.1	21.7	11.3	2.9	0.52

Crud particle size is getting smaller as far from the heated surface. It seems to be caused by a temperature gradient of nanoparticle along the radial direction. It seems like needle-like structure are formed on the bottom layer of the crud. (Fig. 2 (b)) From the point EDX, it is known that Ni/Fe ratio is about 0.5 which means Nickel ferrite deposited majorly. Ni/Fe ratio was slightly increased from cladding to outer surface, however, any noticeable change was not found.

3.2. Structure and chemistry analysis of T2-2 top region

The surface of the area, where the crud was not separated, showed a relatively dense surface, a uniform surface, and no chimney structure was found. The surface of the separated region of the crud was not uniform in the thickness of the crud as before, and the pore estimated as chimney contained in the surface. The size of the crud particles was smaller in the non-separated region, which is similar to the result of past results in which the size of the crud particles decreases as they approach the surface. Therefore, the crud of large particles was relatively porous at the beginning of crud formation, but then the crud with small particle size was deposited at a high density.

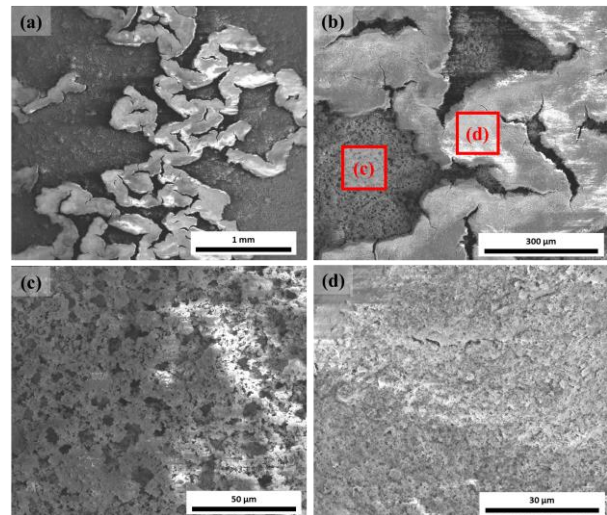


Fig. 3 SEM surface image of T2-2 top specimen in different magnifications

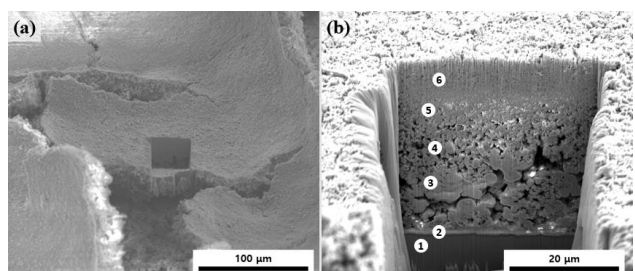


Fig. 4 SEM cross section image of T2-2 top specimen. (a) 52° tilted surface image of FIB milling point and (b) its cross section. Numbers indicate the location that point EDX analysis was conducted.

A ZrO₂ oxide film of about 2.34 μm was grown on the surface of Zr-Nb-Sn alloy, and it was observed that the oxide film had deposited crud. The thickness of the crud at the point is measured as 52.99 μm on average (σ = 0.28). The chemical composition of the upper and lower parts of the EDX was not large, and the Ni / Fe ratio was generally maintained at 0.7 to 0.8.

It appears that the crust of the needle-shaped structure is deposited in a thin region at the bottom nearest to ZrO₂ layer. Thereafter, relatively large particles of the crud were deposited and deposited relatively porous. The size of the crud particles decreases sharply from about 34 to 35 μm from the zirconium oxide film, and the chirped structure inside the crud also disappears. The uppermost deposited crudes appear to have nano-sized particles.

Table 3. Point EDX analysis of the points in Fig. 4 (b) in a.t.%

Point	O	Fe	Ni	Zr	Ni/Fe ratio
1	61.16	8.46	12.87	12.28	-
2	57.74	12.33	5.75	19.74	-
3	57.42	18.09	7.15	14.47	0.40
4	51.25	16.22	11.9	1.58	0.73
5	48.88	18.29	15.55	2.92	0.85
6	52.22	18.09	13.31	1.84	0.74

3.3. Structure and Chemical Composition Change with Heat Flux Condition

From the surface image of the T2-3 specimen, both dense surface region (Fig. 5 (b)) and porous surface region (Fig. 5 (c)) were found. chimney-like structures were formed on the porous surface region and seem to be merged in a circumferential direction.

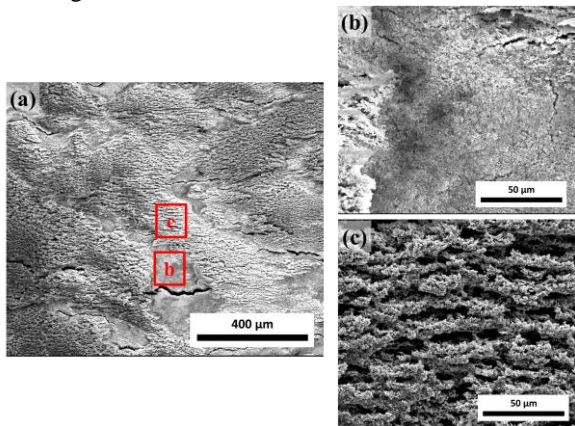


Fig. 5 SEM surface images of T2-3 top specimen in different magnification

Average crud thickness of dense surface region is thinner than that of the porous surface region. The FIB milling was performed at the porous surface region (Fig. 5 (c))

The average thickness of crud is 61.21 μm (σ = 3.289) and average thickness of ZrO₂ is 0.44 μm (σ = 0.09). The crud layer, formed on T2-3 specimen, shows a similar tendency with T2-1 and T2-2 specimen; particle size decreased as it far from the cladding surface. However, in T2-3 there was one more crud layer, which has a proper size of particles and was formed on the surface of crud.

The formation of the third crud layer is related to environmental condition changes during the experiment. During T2-3 experiments, there is a un-boiling period in the middle of the experiment. Due to a serious increase of cladding surface temperature, the inlet coolant temperature was decreased to keep the surface temperature in safety criteria. Excessively decreased coolant temperature made about 1 day of the un-boiling period. After the period coolant temperature increased again and surface temperature was maintained in boiling criteria for the last time. The surface crud layer (third crud layer) seems to be formed after the un-boiling period showing circumferentially merged structure.

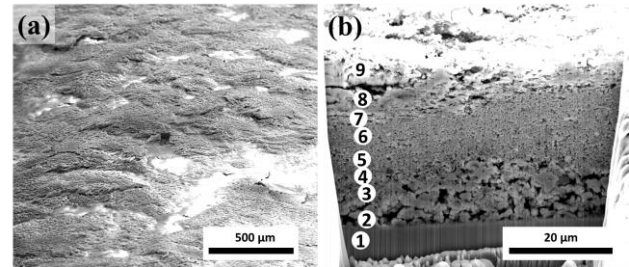


Fig. 6 SEM cross section image of T2-3 specimen. (a) 52° tilted surface images of FIB milling point and (b) its cross section. Numbers indicate the location that point EDX analysis was conducted.

The average thickness of the first crud layer (near cladding), which is composed of relatively large crud particles, was 13.37 μm. The thickness of the dense crud layer (second crud layer) is 23.27 μm on average. the upper porous layer (third layer) ranged from to 0 μm to 37.52 μm, sparsely deposited over a wide area.

Table 4. Point EDX analysis of the points in Fig. 6(b) in a.t.%

Point	O	Fe	Ni	Zr	Ni/Fe ratio
1	42.64	9.9	4.13	43.34	0.417
2	41.40	29.06	16.15	13.39	0.556
3	31.00	46.06	18.75	4.20	0.407
4	28.55	47.17	19.96	4.32	0.423

5	42.14	37.94	15.65	4.27	0.412
6	39.27	40.58	16.61	3.55	0.409
7	32.24	43.81	20.45	3.51	0.467
8	49.24	32.60	15.70	2.45	0.482
9	42.47	37.93	17.59	2.01	0.464

EDS analysis also conducted for T2-3 top specimen in the radial direction. Ni/Fe ratio was about 0.45, which is relatively lower than that of T2-2. The chemical composition does not show any tendency in the radial direction.

3.7. Boron concentration change with crud structure with heat flux.

The boron concentration of each specimen was measured by EDX spectroscopy for the surface of each specimen. Boron concentration did not show any tendency along with heat flux condition. It has the highest value at T2-1 specimen and its lowest value at T2-3 specimen. (Fig. 8)

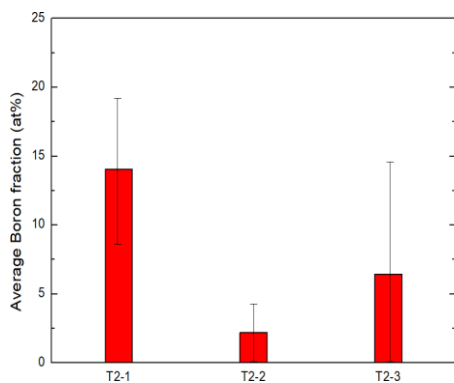


Fig. 7 Boron concentration in crud specimen with different heat flux (T2-1: 46 kW/m², T2-2: 100 kW/m², 150 kW/m²)

From many previous studies, boron accumulation on fuel cladding has been known to relate with boiling behavior at porous crud layer and its structure. [1,4-6] To identify the relationship between boron accumulation and structure of crud, qualitative analysis was performed.

Because the EDX analysis was conducted for the crud surface and its penetration depth is 1 μm, surface porosity and cross-section porosity of upper 10 μm of crud layer were calculated, considering surface roughness of crud. (Fig. 9)

Porosity which is calculated from both cross-section images and surface images show its highest value at T2-1 and show the lowest value at T2-2. The surface porosity of T2-1 is six times higher than that of T2-2 and twice higher than that of T2-3. It shows the same tendency with a boron concentration of each specimen.

This indicates that boron accumulation behavior more actively occurred at the porous crud layer than dense crud layer.

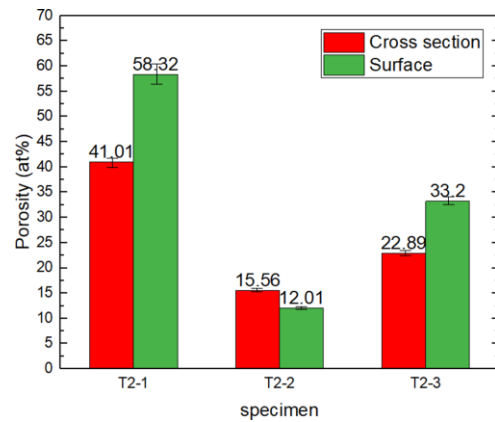


Fig. 8 Crud porosity of each specimens (measured from cross section images (red) and surface images (green))

In the previous study, it was discussed that porosity of crud is inversely proportional to heat flux, however, in T2-3 experiment porosity increased as heat flux increased. Deposition mechanism along heat flux change should be investigated more precisely, however, it is obvious that porosity of crud affects for the chemical concentration of crud.

4. Conclusions

Simulated crud deposition experiments were conducted for various heat flux conditions. To understand the effect of heat flux on crud deposition behavior, structure and chemical composition of crud were investigated using SEM and EDX spectroscopy.

Through the qualitative comparison, it is known that boron concentration increased with the porosity of crud. More quantitative analysis is required for a detail understanding of crud deposition mechanism.

REFERENCES

- [1] T. Alhashan, M. Elforjani, A. Addali, J. Teixeira, Monitoring of bubble formation during the boiling process using acoustic emission signals, *Int. J. Eng. Res. Sci.* 2(4), 66-72, 2016.
- [2] S. H. Baek, H. -S. Shim, J. G. Kim, D. H. Hur, Visualization and acoustic emission monitoring of nucleate boiling on rough and smooth fuel cladding surfaces at atmospheric pressure, *Nucl. Eng. Des.*, 330, 429-436, 2018.
- [3] C. A. Brett, A. O. Brett, *Electrochemistry*, Oxford Univ. Press, New York, 1994.
- [4] J. Deshon, *Simulated Fuel Crud Thermal Conductivity Measurements Under Pressurized Water Reactor Conditions*, TR-1022896, EPRI, Palo Alto, CA.
- [5] D. Hussey, *PWR Axial Offset Anomaly (AOA) Guidelines*, TR-1008102, EPRI, Palo Alto, CA.
- [6] H. Kawamura, H. Kanbe, M. Furuya, H. Kishida, H. Hirano, *Proc. 11th Environ. Deg. Nucl. Mater.*, August 10-14, pp. 617-628, Stevenson, US